Resilient Multi-Hop Autonomous UAV Networks with Extended Lifetime for Multi-Target Surveillance

Abdulsamet Dağaşan, and Ezhan Karaşan, *Member, IEEE*

***Abstract*—Cooperative utilization of Unmanned Aerial Vehicles (UAVs) in public and military surveillance applications has attracted significant attention in recent years. Most UAVs are equipped with sensors and wireless communication equipment with limited ranges. Such limitations pose challenging problems to monitor mobile targets. This paper examines fulfilling surveillance objectives to achieve better coverage while building a resilient network between UAVs with an extended lifetime. The multiple target tracking problem is studied by including a relay UAV within the fleet whose trajectory is autonomously calculated in order to achieve a reliable connected network among all UAVs. Optimization problems are formulated for single-hop and multi-hop communications among UAVs. Three heuristic algorithms are proposed for multi-hop communications and their performances are evaluated. A hybrid algorithm, which dynamically switches between single-hop and multi-hop communications is also proposed. The effect of the time horizon considered in the optimization problem is also studied. Performance evaluation results show that the trajectories generated for the relay UAV by the hybrid algorithm can achieve network lifetimes that are within 95% of the maximum possible network lifetime which can be obtained if the entire trajectories of all targets were known a priori.**

***Index Terms*—UAVs, multi-target surveillance, resilient multi-hop network topology, network lifetime.**

I. Introduction

SURVEILLANCE systems have recently received a significant attention due to the rapid increase in security and safety threats. Some of the surveillance applications include search and rescue operations, monitoring an environment and tracking mobile targets. Among the available surveillance methods, use of Unmanned Aerial Vehicles (UAVs) has been rather widespread for mainly two reasons [1]. Firstly, UAVs can operate where it might be too dangerous for humans to fulfill surveillance duties. Secondly, UAVs can also be operated autonomously without human resource allocation. The rapid advancement in UAV technology has propelled the significance of utilizing cooperative UAVs for tasks related to surveillance [2], tracking [3], and mobile target search [4]. This significance is evident in various applications, particularly in search and rescue operations, where cooperative UAVs are employed for finding and observing targets, in addition to coordinating their flight paths [5]–[7].

The objective of target tracking with cooperative UAVs is to monitor a specific environment and acquire information on the mobile targets. This information is analyzed locally and shared either with a central node or among UAVs. Since the communication ranges of UAVs are limited, connectivity of the UAVs becomes an issue as the mobile targets may move away from each other. Therefore, building a reliable and connected network among UAVs for achieving an extended lifetime is critical.

Effective coordination is fundamental to the success of cooperative UAVs in target tracking. UAV coordination involves methods such as centralization, where a central station manages task distribution and path planning; decentralization, where leader UAVs collaborate on tasks and trajectories; and distributed coordination, where each UAV exercises independent task and trajectory determination [8]–[10]. Additionally, a relay UAV can be used for a successful coordination amongst UAVs [11]. The trajectory planning for relay UAVs is essential for optimizing specific objectives, which involves sophisticated techniques such as Gaussian process models, nonlinear model predictive control, and genetic algorithms [12]–[16]. Various studies explore coordination strategies, such as optimizing network coverage and selecting relay UAVs. Resource optimization and multi-channel, multi-radio models are also under consideration. Particularly in disaster surveillance scenarios, UAV-enabled communication systems, featuring multi-hop and innovative routing algorithms, are developed to enhance overall system performance, specifically for search and rescue operations [16], [17].

This paper proposes trajectory planning algorithms that ensure a connected and robust network topology among distributed cooperative target tracking UAVs with the assistance of a relay UAV. A connected network topology indicates that each UAV in the network has a way of communicating with each other. This study considers both single-hop and multi-hop communication techniques for performing path planning for the relay UAV. In single-hop communication, the relay UAV is directly connected to other UAVs, creating a star topology. On the other hand, in multi-hop communication, the relay UAV can communicate with each UAV through other UAVs, resulting in an arbitrary tree topology. The objective is to maximize the duration for which a connected network topology can be sustained among UAVs.

The main contributions of the study can be listed as follows:

- Trajectory planning algorithms are proposed which ensure a connected and robust network topology among distributed cooperative target tracking UAVs with the

A. Dağaşan and E. Karaşan with the Department of Electrical and Electronics Engineering, Bilkent University, Ankara 06800, Turkey.

assistance of a relay UAV for single and multi-hop communication.
- A probabilistic coverage model is introduced, accounting for UAV position and velocity estimation errors to enhance connectivity predictions. By assigning a probable convex region to each estimated UAV position, the model reflects real-life conditions better and maximises connectivity between UAVs for resilient operations.
- Analyses of network lifetime for two of communication schemes, single-hop and multi-hop, are proposed. For single-hop communication, an algorithm for optimal trajectory planning of relay UAV for extending the lifetime of the network is proposed. For multi-hop communication, three algorithms for optimal trajectory planning of relay UAV for extending the lifetime of the network are proposed. For both communication types, a heuristic approach called "Center of Mass" algorithm is used as a baseline to compare the performances of proposed algorithms.
- Extensive simulations reveal that the proposed algorithms outperform the baseline approach in terms of the maximum possible network lifetime. The most effective algorithm among the proposed algorithms achieves network lifetimes that are within 95% of the maximum lifetime that can be obtained if all target locations were exactly known a priori.

To the best of the authors' knowledge, previous research has not explored the concept of ensuring resilient communication with distributed coordination through the use of a relay UAV which autonomously plans its trajectory for single-hop and multi-hop network topology scenarios. Additionally, this research utilizes a probabilistic coverage model which takes estimation errors in UAV positions into account, which makes it suitable for real-life applications.

The organization of the rest of the article is as follows: Section II provides an overview of the existing research in the field. Section III introduces the system model, position estimator and path planner of relay UAV. In Section IV, the problem formulation of trajectory planning is explained. Section V illustrates the numerical results for the estimator and path planner, respectively. The theoretical limits on network lifetime are discussed in Section VI and the performances of proposed algorithms are compared with these limits. Lastly, Section VII concludes the paper.

II. Related Work

Coordination amongst UAVs is critical for achieving successful cooperative target tracking. Centralized coordination means that UAVs transmit the information to a central station. Task distribution and path planning for each UAV is calculated at the central station and sent back to the on-duty UAVs [8]. Decentralized coordination means there are multiple UAVs that act as central nodes. The information from other UAVs is received by the leader UAVs that cooperatively assign tasks and plan trajectories for the on-duty UAVs [9]. The UAVs can also coordinate in a distributed manner, where each UAV decides its task and plans its trajectory independently [10], [18].

Relay UAVs, acting act as an intermediary bridge between other UAVs or ground-based communication devices are used for enhancing communications between UAVs that may be out of direct range of each other. Regardless of the coordination method, a relay UAV can also be used to achieve reliable target tracking [11]. For the trajectory planning of relay UAV, the task is to plan the path which optimizes a given objective. In [12] path planning for a relay UAV in urban areas for Airborne to Ground (A2G) communications is investigated, where the ground nodes are stationary. A Gaussian process model is formed and it is solved using a Nonlinear Model Predictive Control (NMPC)-based trajectory planner. In [13], the same problem is studied with mobile ground nodes. NMPC-based trajectory planner is also used in this study, however, a discrete genetic algorithm is used to find the optimal control input. To find the optimal path, NMPC is combined with a finite time horizon controlled system. The time horizon defines the period during which the movements of the relay UAV are to be optimized. [14] uses the same NMPC-based planner. However, the objective function is calculated using the concept of Minimum Spanning Tree (MST) which is used to choose the communication link with the highest likelihood for successful transmission. Group of autonomous UAVs for maximizing the network coverage of mobile ground targets is studied in [15] using the game theory, and the performance is compared with the genetic algorithm.

Selection of relay UAVs from a set of cooperative UAVs is suggested in [16]. A matching market-based optimization is presented for different coordination among cooperative UAVs in order to choose relay UAVs. The idea is further extended in [17], where multi-channel, multi-radio competition model is modeled using different objective functions.

Communication coverage amongst UAVs, under communication range restrictions and with multi-hop communication between UAVs and a base station, is studied in [19]. The study focuses on the routing problem in a communication system enabled by UAVs for disaster surveillance. The system includes multiple UAVs that communicate with each other and a remote Terrestrial Base Station (TBS) for aiding search and rescue operations. A novel algorithm called the Multi-hop Opportunistic 3D Routing (MO3DR) is proposed, which addresses coverage and collision constraints without the need for trajectory planning. The aim of the study is to improve the performance of the UAV-enabled communication in disaster scenarios.

The proposed algorithm in [20] is a modular approach for positioning relays and planning trajectories for UAV missions. It ensures that the UAV mission team maintains connectivity with minimal relays and feasible paths. The study presents different strategies for relay positioning and compares them with ideal and Voronoi-based benchmark schemes. The concept is further developed in [21] by introducing dynamic relay selection from a group of available UAVs.

The problem of network connectivity has been extensively studied; however, several key innovations are introduced in this work. Positioning uncertainties, which are inherent in real-world UAV operations, are introduced to the problem formulation for narrowing the gap between the literature

and real-life applications. Additionally, both single-hop and multi-hop communication scenarios are addressed, providing a comprehensive and adaptable solution for various operational contexts. This dual approach, uncommon in the literature, offers practical insights into the trade-offs and advantages of each communication type. The proposed algorithms are benchmarked against a heuristic approach, ensuring that the solutions are both theoretically sound and practically viable. Furthermore, the algorithms are designed to maximize the network's operational lifespan under dynamic conditions, ensuring sustained connectivity and robustness. This focus on longevity and robustness under uncertainty significantly extends the existing research.

III. System Model

A target tracking system is considered, where mobile targets are surveilled by a team of N UAVs, requiring connectivity to be maintained throughout the mission. Connectivity among the UAV team is enhanced by a relay UAV. The path of the relay UAV is autonomously decided for ensuring continuous connectivity with the other UAVs. The system primarily comprises five components: Firstly, the mobility model for the targets is described by the target motion model. Information on the targets is gathered by the tracker, allowing the UAV to adjust its speed and turn angle for optimal tracking. The mobility model of the UAVs is explained by the UAV motion model. The positions and velocities of the tracker UAVs are determined by the estimator. Finally, the optimal trajectory for the relay UAV is found by the path planner using the estimation data. The system model is depicted in Figure 1.

There are some assumptions which are essential for the system model that are listed as follows:

- IMU and GNSS sensors on the tracker UAVs, along with the GNSS receiver on the relay UAV, provide accurate and timely position and velocity data. Each target is tracked by a UAV, which directly observes the current state of the target using its own sensors.
- It is assumed that the communication between the relay UAV and the tracker UAVs occurs under line-of-sight conditions, which is a realistic assumption for UAV-to-UAV communication. For the communication model, the disc model approach is chosen due to its simplicity and suitability for UAV-to-UAV communication, which typically occurs under line-of-sight conditions [22].
- UAVs are assumed to have fixed wings, imposing limitations on acceleration and turn angles. Additionally, the altitude of the UAVs is constant, so the z-coordinate is omitted from the system models.
- The communication range of both the relay UAV and the tracker UAVs is limited, necessitating careful path planning for maintaining connectivity.
- The system is formulated using a discrete-time model.

In the discrete-time model, k^{th} time step corresponds to the sample at time $k\Delta t$, where Δt is the sampling period. Parameters related to target $i \in \{1, 2, \ldots, N\}$ are denoted with the T_i superscript, e.g. $x_k^{T_i}$, which represents the state of i^{th} target. Parameters related to UAV $i \in \{1, 2, \ldots, N\}$ are denoted with the U_i superscript, e.g. $x_k^{U_i}$, which corresponds to the state of i^{th} UAV. Parameters related to the relay UAV are denoted with the U_0 superscript, e.g. $x_k^{U_0}$ which indicates the state of the relay UAV.

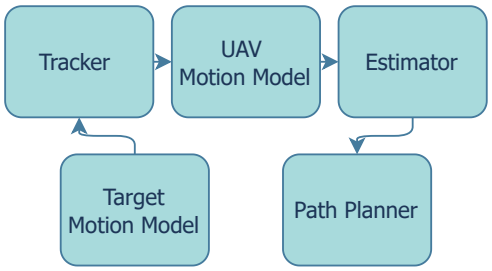

Fig. 1. System Model.

A. Target Motion Model

Successful target tracking depends on accurately extracting information about the target's state from sensor observations. The target motion should be modeled in a manner that allows for easy extraction of this information [23]. In this system, target tracking involves observing a moving target through sensors and using airborne computers to process the signals from these sensors. This process allows for the perception of the target's environment and the making of tracking decisions accordingly [24].

For the target tracking, constant velocity (CV) and constant turn (CT) models are available in the literature [23]. CV motion is a non-manuevering motion that is straight and linear with a constant velocity. On the other hand CT model represents the motion of a model that have a constant speed and constant turn rate.

Discrete-time state-space model of the CT motion can be written as follows [25]:

$$\mathbf{x}_{k+1}^{T_i} = \mathbf{F}\mathbf{x}_k^{T_i} + \mathbf{G}\boldsymbol{\eta}_k, \tag{1}$$

where $\mathbf{x}_k^{T_i}$ is the target state vector of i^{th} target. $\mathbf{F}$ is the state transition matrix, $\mathbf{G}$ is the disturbance matrix and $\boldsymbol{\eta}_k$ is the process noise. The state vector comprises of target position and velocity vectors $\mathbf{p}_k^{T_i}, \mathbf{v}_k^{T_i}$, respectively and can be written as follows:

$$\begin{aligned} \mathbf{x}_k^{T_i} &= [\mathbf{p}_k^{T_i}, \mathbf{v}_k^{T_i}]^{\mathbf{T}}, \\ \mathbf{p}_k^{T_i} &= [p_{x,k}^{T_i}, p_{y,k}^{T_i}]^{\mathbf{T}}, \\ \mathbf{v}_k^{T_i} &= [v_{x,k}^{T_i}, v_{y,k}^{T_i}]^{\mathbf{T}}, \end{aligned} \tag{2}$$

where $p_{x,k}^{T_i}$, $p_{y,k}^{T_i}$ corresponds to positions in the x and y directions of i^{th} target at time step k, respectively and $v_{x,k}^{T_i}$, $v_{y,k}^{T_i}$ represent velocities in the x and y directions of i^{th} target at time step k and $\mathbf{T}$ denotes the transpose operation for the rest of the paper. The measurement equation of i^{th} target can be written as:

$$\mathbf{z}_k^{Ti} = \mathbf{H}\mathbf{x}_k^{T_i} + \boldsymbol{\zeta}_k \tag{3}$$

where $\mathbf{z}_k^{Ti}$ is the received measurement, $\mathbf{H}$ is the measurement matrix and $\boldsymbol{\zeta}_k$ is the measurement noise. For CV models with

known turn rate ω following state transition matrix $\mathbf{F}$ is used [25]:

$$\mathbf{F} = \begin{bmatrix} 1 & \frac{\sin(\omega\Delta t)}{\omega} & 0 & -\frac{1-\cos(\omega\Delta t)}{\omega} \\ 0 & \frac{1-\cos(\omega\Delta t)}{\omega} & 1 & \frac{\sin(\omega\Delta t)}{\omega} \\ 0 & \cos(\omega\Delta t) & 0 & -\sin(\omega\Delta t) \\ 0 & \sin(\omega\Delta t) & 0 & \cos(\omega\Delta t) \end{bmatrix}. \tag{4}$$

For $\mathbf{G}$, $\mathbf{H}$ matrices and $\boldsymbol{\eta}_k$, $\boldsymbol{\zeta}_k$ noises, the system model in [25] used.

B. Kinematics of UAVs

A constant-altitude kinematic model is used for the relay UAV, considering its physical constraints [26]. With sampling period Δt, the discrete kinematic model for i^{th} UAV as follows

$$\begin{aligned} p_{x,k}^{U_i} &= p_{x,k-1}^{U_i} + v_{k-1}^{U_i}\cos\theta_{k-1}^{U_i}\Delta t, \\ p_{y,k}^{U_i} &= p_{y,k-1}^{U_i} + v_{k-1}^{U_i}\sin\theta_{k-1}^{U_i}\Delta t, \\ v_k^{U_i} &= v_{k-1}^{U_i} + a_k^{U_i}\Delta t, \\ \theta_k^{U_i} &= \theta_{k-1}^{U_i} + \omega_k^{U_i}\Delta t, \end{aligned} \tag{5}$$

where $p_{x,k}^{U_i}, p_{y,k}^{U_i}$ corresponds to positions in the x, y directions and $v_{x,k}^{U_i}$, $v_{y,k}^{U_i}$ are velocities in the x and y directions, $a_k^{U_i}$, $\theta_k^{U_i}$ and $\omega_k^{U_i}$ are acceleration, bank angle and turn rate of i^{th} UAV at time step k, respectively.

Kinematic model of UAVs in (5) is constrained by practical limitations which are identical for both UAVs. The required control input of i^{th} UAV consists of the speed increment and the turn rate is

$$\mathbf{u}_k^{U_i} = [a_k^{U_i}, \omega_k^{U_i}]^{\mathbf{T}} \in \mathbb{R}^2. \tag{6}$$

The limitations apply at each step k on the speed and on the control input of UAVs.

$$\begin{aligned} v_{min} \leq v_k^{U_i} \leq v_{max}, \\ \omega_{min} \leq w_k^{U_i} \leq \omega_{max}, \\ a_{min} \leq a_k^{U_i} \leq a_{max}. \end{aligned} \tag{7}$$

For this model we can write the UAV state vector for i^{th} UAV, $\mathbf{x}_k^{U_i}$, as similar to the model in (2).

$$\begin{aligned} \mathbf{x}_k^{U_i} &= [\mathbf{p}_k^{U_i}, \mathbf{v}_k^{U_i}]^{\mathbf{T}}, \\ \mathbf{p}_k^{U_i} &= [p_{x,k}^{U_i}, p_{y,k}^{U_i}]^{\mathbf{T}}, \\ \mathbf{v}_k^{U_i} &= [v_{x,k}^{U_i}, v_{y,k}^{U_i}]^{\mathbf{T}}, \end{aligned} \tag{8}$$

where UAV position and velocity vectors $\mathbf{p}_k^{U_i}, \mathbf{v}_k^{U_i}$, respectively. Note that $v_{x,k}^{U_i} = v_k^{U_i}\cos\theta_k^{U_i}$ and $v_{y,k}^{U_i} = v_k^{U_i}\sin\theta_k^{U_i}$. For relay UAV, $\mathbf{x}_k^{U_0}$ is used.

C. Tracker

The target tracking problem is defined using the state vectors of targets and UAVs. The objective is to minimize the distance between UAVs and targets so the optimization problem can be formulated as follows [27]:

$$\begin{aligned} \min_{\mathbf{u}_k^{U_i}} \quad & \sum_{i=1}^{N} \|\boldsymbol{\alpha} \circ (\mathbf{x}_k^{U_i} - \mathbf{z}_k^{T_i})\| \\ \text{s.t.} \quad & (5), (6), (7), (8) \end{aligned} \tag{9}$$

where $\boldsymbol{\alpha} \in \mathbb{R}^4$. $\boldsymbol{\alpha}$ is the weight parameter to adjust the focus of the optimization problem on different objectives and $\circ$ represents the Hadamard product. Received measurement vector is used in the formulation instead of the state vector, since the state vector is unknown to the UAV. State vectors also include the velocity vectors.

D. Position Estimator

In order to estimate the tracker UAV positions, Kalman Filter is utilized [28]. Relay UAV calculates the tracker UAV states at time step $k+1$ with the information it received from the tracker UAV sensors at time step k.

The state prediction stage can be written as:

$$\hat{\mathbf{x}}_k^{U_i} = \begin{bmatrix} \hat{\mathbf{p}}_k^{U_i} \\ \hat{\mathbf{v}}_k^{U_i} \end{bmatrix} = \begin{bmatrix} \mathbf{p}_{k-1}^{U_i} + \mathbf{v}_{k-1}^{U_i}\Delta t + \frac{1}{2}\widetilde{\mathbf{a}}_{k-1}^{U_i}\Delta t^2 \\ \mathbf{v}_{k-1}^{U_i} + \widetilde{\mathbf{a}}_{k-1}^{U_i}\Delta t \end{bmatrix}. \tag{10}$$

$\hat{\mathbf{x}}_k^{U_i}$ is the predicted state vector with similar construction to (8). $\widetilde{\mathbf{a}}_k^{U_i}$ is the estimated acceleration vector which includes acceleration values in Cartesian coordinates and $\mathbf{a}_k^{U_i}$ is the estimated acceleration vector which includes acceleration values in Cartesian coordinates. The state prediction equation can be rewritten as:

$$\hat{\mathbf{x}}_k^{U_i} = \begin{bmatrix} \mathbf{I} & \mathbf{I}\Delta t \\ \mathbf{0} & \mathbf{I} \end{bmatrix} \mathbf{x}_{k-1}^{U_i} + \begin{bmatrix} \frac{1}{2}\mathbf{I}\Delta t^2 \\ \mathbf{I}\Delta t \end{bmatrix} \widetilde{\mathbf{a}}_{k-1}^{U_i}. \tag{11}$$

where $\mathbf{I}$ represents 2×2 identity matrix and $\mathbf{0}$ represents the 2×2 zero matrix.

The process noise on the acceleration vector can be written with its zero mean Gaussian noise vector $\boldsymbol{\psi}_k$.

$$\widetilde{\mathbf{a}}_{k-1}^{U_i} = \mathbf{a}_{k-1}^{U_i} + \boldsymbol{\psi}_{k-1}, \tag{12}$$

The system model is given by:

$$\hat{\mathbf{x}}_k^{U_i} = \mathbf{A}\mathbf{x}_{k-1}^{U_i} + \mathbf{B}\mathbf{a}_{k-1}^{U_i} + \boldsymbol{\psi}_{k-1}, \tag{13}$$

where,

$$\mathbf{A} = \begin{bmatrix} \mathbf{I} & \mathbf{I}\Delta t \\ \mathbf{0} & \mathbf{I} \end{bmatrix}, \tag{14}$$

$$\mathbf{B} = \begin{bmatrix} \frac{1}{2}\mathbf{I}\Delta t^2 \\ \mathbf{I}\Delta t \end{bmatrix}^{\mathbf{T}}. \tag{15}$$

The following equation can be written for the measurement vector $\mathbf{z_k}$:

$$\mathbf{z}_k^{Ui} = \mathbf{M}\mathbf{x}_k^{U_i} + \boldsymbol{\xi}_k \tag{16}$$

where $\boldsymbol{\xi}_k$ is the measurement sensor noise at time step k. For the measurement parameters $\mathbf{M}$, $\boldsymbol{\xi}_k$ please check [28].

The tracker UAV positions can be estimated using the Kalman Filter. The estimates, along with a probability parameter, are utilized for computing the cost function in the optimization problem.

E. Path Planner

In order to create a connected network between UAVs, a dynamic optimization problem is solved by the relay UAV to determine its own path autonomously. The aim is to create a connected network within a designated time frame denoted as $[0, T]$. However, solving the optimization problem at the beginning is not feasible due to the high computational complexity and time constraints, particularly for larger values of T. Moreover, it is essential to consider environmental changes, target paths, and UAV paths. Therefore, a receding horizon approach is used.

The estimator is utilized to estimate the UAV positions within a certain time frame $[k, k+E\Delta t]$ where $E\Delta t$ represents the estimation window's duration. A path planning strategy is created for a specific duration of $[k, k + W\Delta t]$, where the optimization horizon window's duration, denoted as $W\Delta t$, is utilized to ensure that the UAVs remain connected for as long as possible. The selection of W and E is such that they are positive integers ($W, E \in \mathbf{Z^{0+}}$) and that W is a factor of E, i.e., $W \mid E$. If $W = 1$, the optimization problem is referred to as the *no horizon problem*, as the objective function is solved only to obtain the current time solution. Relay UAV estimates the positions of tracker UAVs beforehand for a period of time ($E\Delta t$), then the optimization problem for path planning is solved for each ($W\Delta t$) time duration.

The aim of the optimization problem is to find the optimal input vector $\overset{*}{\mathbf{u}}_k^{U_0} \in U$ which maximizes the probability that the network topology is connected at time step k. U represents the set of possible inputs under the restrictions of (7). For arbitrary time step k_0, given the variable $\overset{*}{\mathbf{u}}_k^{U_0}$ for the interval $k \in [k_0, k_0 + W\Delta t]$, the optimal state parameter $\overset{*}{\mathbf{x}}_k^{U_0}$ can be found.

A discrete-time version of the dynamic optimization problem can be formulated similar to a Bolza-type Optimal Control Problem (OCP) [29]. The Lagrange term can be defined as:

$$\Phi_L(k, \mathbf{u}) = \rho(k, \mathbf{x}_k^{U_0}, \mathbf{u}_k^{U_0}), \tag{17}$$

where $\rho(k, \mathbf{x}_k^{U_0}, \mathbf{u}_k^{U_0})$ denotes the probability of having a connected network topology with state $\mathbf{x}_k^{U_0}$ at time step k. The Mayer term can be written as:

$$\Phi_M(k) = d(\mathbf{x}_{k_0+W\Delta t}^{U_0}, \mathbf{x}_{k_0+W\Delta t}^{U_1}, \ldots, \mathbf{x}_{k_0+W\Delta t}^{U_N}), \tag{18}$$

where $d(\mathbf{x}_{k_0+W\Delta t}^{U_0}, \mathbf{x}_{k_0+W\Delta t}^{U_1}, \ldots, \mathbf{x}_{k_0+W\Delta t}^{U_N})$ is a function of distance between UAVs for at the end of the optimization horizon for $k \in [k_0, k_0 + W\Delta t]$. The resulting optimization problem is given by:

$$\begin{aligned} \max_{\mathbf{u}_k^{U_0}} \quad & \rho(k, \mathbf{x}_k^{U_0}, \mathbf{u}_k^{U_0}) + \\ & d(\mathbf{x}_{k_0+W\Delta t}^{U_0}, \mathbf{x}_{k_0+W\Delta t}^{U_1}, \ldots, \mathbf{x}_{k_0+W\Delta t}^{U_N}) \\ \text{s.t.} \quad & (5), (6), (7), (8) \\ & k \in [k_0, k_0 + W\Delta t] \end{aligned} \tag{19}$$

The objective of the task is to select the optimal values of $a_k^{U_0}$ and $\omega_k^{U_0}$ for a given interval $k \in [k_0, k_0 + W\Delta t]$ that maximize the objective function. In order to assess the effect of the optimization horizon, the optimization problem is also solved for $W = 1$, which corresponds to solving for a sampling period of Δt. The objective function $\Phi_L(k, \mathbf{u}) + \Phi_M(k)$ varies depending on the type of the network: single-hop or multi-hop communication.

IV. Problem Formulation

A. Single-Hop Communication

In this section, tracker UAVs and the relay UAV should be able to communicate with a single-hop communication. All the tracker UAVs should be connected to the relay UAV directly. To check the connectivity between relay UAV and the tracker, the distance parameter is defined as:

$$d_i(k) = ||\mathbf{p}_k^{U_0} - \mathbf{p}_k^{U_i}||_2, \tag{20}$$

where $d_i(k)$ is the distance between i^{th} tracker UAV and relay UAV at time step k.

In order to model the inaccuracy in estimating the velocity and position of UAVs, a probabilistic model is used as opposed to a deterministic model. A probable convex region is assigned to the estimated UAV to guarantee the maximization of the connectivity between UAVs. In this case, a circular region is assigned with radius $r_i(k) = m \cdot \mathbf{v}_k^{U_i}$ and center $\mathbf{p}_k^{U_i}$ to a tracker UAV. Assuming a uniformly distributed position error, the intersection area between the circular UAV position uncertainty region and the area corresponding to the communication range is calculated to get the connectivity likelihood function $I(R, r, l)$. The visualization for an example scenario is shown in Figure 2.

The intersection area $I(R, r, d)$ between two circles can be found as:

$$\begin{aligned} & I(R, r, d) = \\ & R^2 \arccos\left(\frac{R^2 - r^2 + d^2}{2dR}\right) + r^2 \arccos\left(\frac{r^2 - R^2 + d^2}{2dr}\right) \\ & -\frac{1}{2}\left((R+r+d)(R-r+d)(-R+r+d)(R+r-d)\right)^{1/2}, \end{aligned} \tag{21}$$

where R and r are the radii of two circles and d is the distance between the centers of two circles.

The probability of connectivity for UAV i, denoted as ρ_i, is expressed as the ratio of the intersection area between the circular regions of the tracker UAV and the relay UAV, to the total area of the circular region of the tracker UAV.

$$\rho_i(k, \mathbf{x}_k^{U_0}, \mathbf{u}_k^{U_0}) = \begin{cases} \frac{I(R, r_i(k), d_i(k))}{\pi r_i(k)^2}, & \text{if } d_i(k) \leq R + r_i(k) \\ 0, & \text{otherwise.} \end{cases} \tag{22}$$

By using the independence assumption for connectivity of individual UAVs and position errors between different UAVs, the overall probabilistic connectivity function ρ can be written in the product form. The probability that all tracker UAVs are connected to the relay UAV can be expressed as follows:

$$\rho(k, \mathbf{x}_k^{U_0}, \mathbf{u}_k^{U_0}) = \prod_{i=1}^{N} \rho_i(k, \mathbf{x}_k^{U_0}, \mathbf{u}_k^{U_0}), \tag{23}$$

.

In single-hop communication, it is necessary for the relay UAV to establish a direct connection with the tracker UAVs.

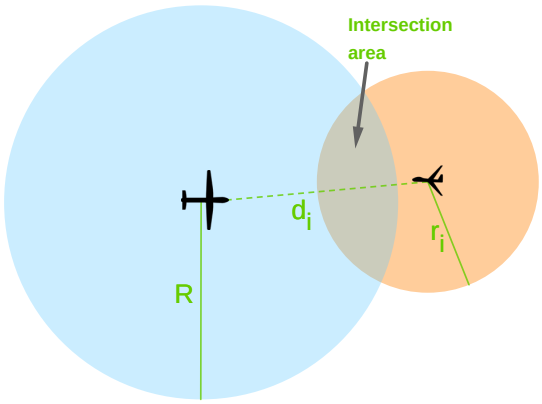

Fig. 2. Blue circle is the communication area of the relay UAV and the orange circular region is the estimated UAV position area. If the tracker UAV is within the intersection of these circles, it can communicate with the relay UAV. Otherwise, it cannot. The position error of the tracker UAV is assumed to be uniformly distributed, and the probability of connectivity is determined by calculating the intersection area between the circle corresponding to the relay UAV's communication range and the circle corresponding to the tracker UAV's estimated position. The radius of tracker UAV's position uncertainty depends on its speed.

The proposed approach involves closely monitoring each tracker UAV to accommodate any changes in their movements. For this purpose, $d(\mathbf{x}_{k_0}^{U_0}, \mathbf{x}_{k_0}^{U_1}, \ldots, \mathbf{x}_{k_0}^{U_N})$, is utilized which aims to minimize the maximum distance between the relay UAV and the tracker UAVs. In order to avoid this component dominating the objective function, it is multiplied by a small value of ϵ, $0 < \epsilon << 1$. The function can be expressed as follows:

$$d(\mathbf{x}_{k_0}^{U_0}, \mathbf{x}_{k_0}^{U_1}, \ldots, \mathbf{x}_{k_0}^{U_N}) = -\epsilon \cdot \max\{d_i(k_0)\}. \tag{24}$$

The resulting optimization problem is expressed as:

$$\begin{aligned} \max_{\mathbf{u}_k^{U_0}} \quad & \prod_{i=1}^{N} \rho_i(k, \mathbf{x}_k^{U_0}, \mathbf{u}_k^{U_0}) - \epsilon \cdot \max\{d_i(k_0)\} \\ \text{s.t.} \quad & (5), (6), (7), (8) \\ & k \in [k_0, k_0 + W\Delta t] \end{aligned} \tag{25}$$

While the primary objective is to maximize the probability that the relay is connected to all tracker UAVs, the secondary objective is used to make sure that among all solutions that optimize the primary objective, the one which minimizes the maximum distance between the relay and tracker UAVs is chosen. The path planner component solves this optimization problem with the given position estimates of the other UAVs in a chosen horizon window and generates the trajectory.

B. Multi-Hop Communication

Within this section, multi-hop communication is utilized by the tracker UAVs and the relay UAV, meaning that direct connection between them is not required. Instead, the goal is to establish a connected network topology among all N UAVs. To solve the dynamic optimization problem, the objective function defined in (19) is employed. The Lagrange term $\rho(k, \mathbf{x}_k^{U_0}, \mathbf{u}_k^{U_0})$ and the Mayer term $d(\mathbf{x}_{k_0+W\Delta t}^{U_0}, \mathbf{x}_{k_0+W\Delta t}^{U_1}, \ldots, \mathbf{x}_{k_0+W\Delta t}^{U_N})$ of the objective function $\Phi_L(k, u) + \Phi_M(k)$ will differ from those used in the context of single-hop communication.

Multi-hop communication is established by creating a network graph consisting of $N+1$ UAVs, including the relay UAV, where each UAV is represented as a node in the graph. For all possible $\binom{N+1}{2}$ edges, a state matrix $\mathbf{S}$ is defined to calculate the probabilistic connectivity function ρ. The state matrix contains all possible combinations of edges that can be connected. Consequently, the size of the state matrix $\mathbf{S}$ is $\binom{N+1}{2} \times 2^{\binom{N+1}{2}}$. To calculate the probability of a connected network, the connectivity probability for each edge is computed, and then multiplied with the state matrix to obtain the value of the probabilistic connectivity function ρ.

The connectivity probability for each edge is determined by calculating the average intersection area between each UAV, utilizing the same model depicted in Figure 2. For edges connecting the relay UAV to other UAVs, the probability of connection derived in (22) is used. However, for network edges connecting two tracker UAVs, a different probabilistic model is employed due to position inaccuracy being valid for both UAVs. Thus, an average intersection area between tracker UAVs i and j is computed to determine the probability of establishing a link between UAVs i and j.

The Probability Density Function (PDF) of distance between two tracker UAVs, $f(x; d, r)$, can be geometrically formulated as:

$$f(x; d, r) = \frac{2x}{\pi r^2} \arccos\left(\frac{x^2 - r^2 + d^2}{2dx}\right). \tag{26}$$

The average intersection area can be found as follows:

$$I_{ij}(k) = \int_{d_{ij}(k)-r_i(k)}^{d_{ij}(k)+r_i(k)} I(R, r_i(k), x) f(x; d_{ij}(k), r_j(k)) dx \tag{27}$$

where $I(R, r_i(k), x)$ is the intersection area between UAV j with communication radius R and UAV i with location region with radius $r_i(k)$ at time step k. It is assumed that all tracker UAVs possess the same communication radius R. The average intersection area is calculated by integrating over the distance $d_{ij}(k) - r_j(k) \leq x \leq d_{ij}(k) + r_j(k)$ between two UAVs.

By applying (27) to each pair of vertices in the matrix, vector $\boldsymbol{\iota}_k$ of size $1 \times \binom{N+1}{2}$ is derived. This vector is multiplied with the state matrix $\boldsymbol{S}$ to obtain a vector of size $1 \times 2^{\binom{N+1}{2}}$ which contains the probabilities for all possible network configurations. The transpose of this vector is multiplied with the one vector $\mathbb{1}_{1 \times 2^{\binom{N+1}{2}}}$ to determine the probabilistic connectivity function.

$$\rho(k, \mathbf{x}_k^{U_0}, \mathbf{u}_k^{U_0}) = \mathbb{1}(\boldsymbol{\iota}_k \mathbf{S})^{\mathbf{T}}. \tag{28}$$

The relay UAV is responsible for establishing a connected network in multi-hop communication. Three algorithms are proposed to enable the relay UAV to strategically position itself and sustain connectivity for longer periods while UAV positions change over time.

1) Nearest Point Algorithm: The first algorithm involves dividing the UAVs into two sets, denoted as S_1 and S_2. The UAV furthest away from the other UAVs is placed in S_1, while the rest of the UAVs are in S_2. The distances of all UAVs in both sets to the relay UAV are measured, and the closest ones are selected. Let UAV $U_k \in S_1$ and UAV $U_l \in S_2$

be the closest to the relay UAV, with distances $d_k(k)$ and $d_l(k)$, respectively. In the next iteration, the control input that minimizes $\max\{d_k(k), d_l(k)\}$ is chosen. To prevent this part from dominating the objective function, it is multiplied by a small $\epsilon > 0$ value. This can be used as the Mayer part of the optimal control problem as follows:

$$d(\mathbf{x}_{k_0}^{U_0}, \mathbf{x}_{k_0}^{U_1}, \ldots, \mathbf{x}_{k_0}^{U_N}) = -\epsilon \cdot \max\{d_k(k), d_l(k)\} \quad (29)$$

The objective function of the resulting optimization problem can be written as:

$$\begin{aligned} \max_{\mathbf{u}_k^{U_0}} \quad & \mathbb{1}(\boldsymbol{\iota}_k \mathbf{S})^T - \\ & \epsilon \cdot \max\{d_k(k_0 + W\Delta t), d_l(k_0 + W\Delta t)\} \quad (30) \\ \text{s.t.} \quad & (5), (6), (7), (8) \\ & k \in [k_0, k_0 + W\Delta t] \end{aligned}$$

2) Midpoint Algorithm: In this algorithm, the centroid of the positions of UAVs in S_2 is first calculated and denoted by $\mathbf{p}_{mean,k}$. Next, the distance between the relay UAV and $\mathbf{p}_{mean,k}$ is calculated and denoted as $d_{mean}(k)$.

$$d_{mean}(k) = ||\mathbf{p}_k^{U_0} - \mathbf{p}_{mean,k}||_2. \quad (31)$$

The control input is selected to minimize $\max\{d_{mean}(k), d_k(k)\}$ in this algorithm. To prevent this part from dominating the objective function, it is multiplied by a small $\epsilon > 0$ value. This can be utilized as the Mayer part of the OCP as follows:

$$d(\mathbf{x}_{k_0}^{U_0}, \mathbf{x}_{k_0}^{U_1}, \ldots, \mathbf{x}_{k_0}^{U_N}) = -\epsilon \cdot \max\{d_k(k), d_{mean}(k)\} \quad (32)$$

The objective function of the optimization problem can be expressed as:

$$\begin{aligned} \max_{\mathbf{u}_k^{U_0}} \quad & \mathbb{1}(\boldsymbol{\iota}_\mathbf{k} \mathbf{S})^T - \\ & \epsilon \cdot \max\{d_k(k_0 + W\Delta t), d_{mean}(k_0 + W\Delta t)\} \quad (33) \\ \text{s.t.} \quad & (5), (6), (7), (8) \\ & k \in [k_0, k_0 + W\Delta t] \end{aligned}$$

3) Hybrid Algorithm: A hybrid approach is employed in the last algorithm, which dynamically switches between single-hop and multi-hop objectives. The algorithm prioritizes single-hop communication and solves the optimization problem introduced in (25) if single-hop communication is possible. If the obtained solution does not satisfy the following conditions:

$$\max_{\mathbf{u}_k^{U_0}} \prod_i^N \rho_i(k, \overset{*}{\mathbf{x}}_k^{U_0}, \overset{*}{\mathbf{u}}_k^{U_0}) \geq 0, \quad (34)$$

single-hop connectivity is not achieved, hence the algorithm switches to multi-hop communication optimization problem. The optimization problem in (33) is then solved to obtain the optimal trajectory.

V. Performance Analysis

The scenario under consideration involves a group of three tracker UAVs, each tasked with observing a moving target. In addition to these tracker UAVs, a relay UAV is employed, which autonomously positions itself to extend the network's operational lifetime. The performance of the system is evaluated across several dimensions, including the accuracy of the position estimator, the efficiency of the tracker, and the effectiveness of the path planner. Furthermore, simulation results are presented for both single-hop and multi-hop communication scenarios, providing a comprehensive assessment of the communication strategies employed in the network. The general simulation parameters can be seen in Table I.

TABLE I
General Simulation Parameters

Parameters	Value	Description
T	10240	Number of time steps (Δt)
Δt	1	Time between time steps (s)
N	3	Number of UAVs
m	10	Probability multiplier of UAVs
N_{sim}	20	Number of different simulations

TABLE II
Target motion model parameters.

Parameters	Target 1	Target 2	Target 3
$\mathbf{p}_0^{T_i}$ (m)	[0,0]	[500, 500]	[1000, 1000]
$v_0^{T_i}$ (m/s)	35	30	25
ω	$45°$	$0°$	$-90°$
$\Delta\omega$	128	128	256
ω_{min}	$0°$	$-15°$	$-15°$
ω_{max}	$7.5°$	$15°$	$15°$

A. Target Motions and Target Tracking

There are three targets, each employing a stochastic CV and CT mobility model. Each target begins from a unique initial position and moves in different directions. Two of the targets adjust their heading angle every 2 minutes, while the third target changes its angle every 4 minutes. This periodic change in angle is represented by the parameter $\Delta\omega$ in Table II. The detailed hyperparameters used in the simulation are also presented in Table II.

The trajectories of the targets, along with their respective tracker UAVs, are depicted in Figure 3. Tracker UAV trajectories are generated with the formulated optimization problem in Section II and parameters in Table III are used. If two possible state vectors give equal objective function, it would be better to try to match the velocity of the target. For this reason $\boldsymbol{\alpha} = [0.99, 0.99, 0.01, 0.01]$ is used for the objective function.

Due to the initial positions and the inherent noise in the system, tracking errors are observed, as illustrated in Figure 4a. Although the tracking performance is not perfect, it is sufficient to create a realistic scenario where extending the network's operational lifetime proves beneficial. In this scenario, UAVs must communicate with each other to successfully execute the mission.

B. Estimation of Tracker UAVs

A Monte Carlo simulation is conducted with $M = 100$ to assess the robustness of the filter. The Root Mean Square Error (RMSE) values obtained for the estimated position and velocity are presented in Figure 4b. The plot reveals

TABLE III
TRACKER UAV PARAMETERS.

Parameter	Value	Description
R (m)	$\{50, 100, 150, 200\}$	Communication range
$\mathbf{p_0^{U_i}}$ (m)	[166.3, 500]	Initial position
$\mathbf{v_0^{U_i}}$ (m/s)	[25, 25]	Initial velocity
$\theta_0^{U_i}$	$0°$	Initial heading angle
v_{min} (m/s)	20	Minimum velocity
v_{max} (m/s)	40	Maximum velocity
ω_{min}	$-15°$	Minimum turn rate
ω_{max}	$15°$	Maximum turn rate

that the average RMSE values for the estimated quantities converge after some time. The error in position estimation is approximately 2 [m], whereas the error in velocity estimation is less than 0.03 [m/s]. This means the position and velocity estimation of the tracker UAVs are successful and will not affect the outcome of the path planner.

C. Path Planning

Different multiple scenarios with various setups were simulated to assess the performance of the path planner for both single and multi-hop communication. General simulation parameters can be seen in Table I. For the path planner specific parameters, please check IV.

A center of mass [30] approach is used as a baseline, where the UAV trajectory is chosen as the centroid of the three targets at time t. The results of the center of mass approach are treated as the baseline to compare with the optimization problem results. The calculated trajectories of the relay UAV are displayed for the scenario shown in Figure 5.

The trajectory of the relay UAV optimized for the single-hop communication objective is shown in Figure 5a. The movements of UAVs 2 and 3 are almost symmetric on the $x = y$ line, and due to the motion of UAV 1, the center of mass trajectory has a similar shape. Conversely, the relay

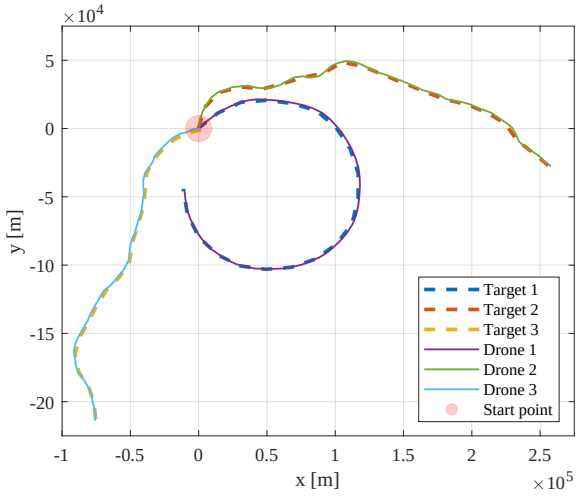

Fig. 3. Tracker UAV trajectories.

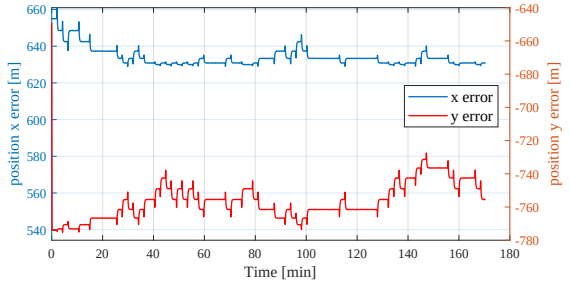

(a) Tracking error between UAV 3 and Target 3 positions.

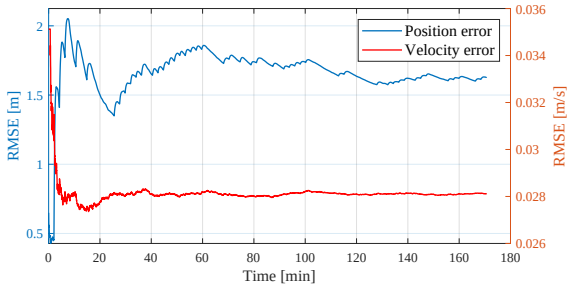

(b) RMSE values for the position and velocity estimation obtained by Monte Carlo simulations.

Fig. 4. Comparison of tracking and estimation errors.

UAV algorithm for the single-hop communication scenario attempts to establish a connection with the furthest UAV. Its trajectory shows an effort to maintain a connection with UAVs 2 and 3 since it is connected to UAV 1. However, since the algorithm does not take future positions into account without an optimization horizon, it fails to keep up with the tracker UAVs, unlike in the case where an optimization horizon is present.

The trajectory resulting from the nearest point algorithm in the multi-hop communication scenario is depicted in Figure 5b. Among the UAVs, UAV 3 is the furthest, while UAV 1 and UAV 2 are in proximity to each other. Within this set, UAV 1 is closer to the relay UAV. Thus, the relay UAV stays in the centroid of UAV 1 and UAV 3, using UAV 1 to establish communication with UAV 2. As UAV 3 moves farther away, the relay UAV adjusts its trajectory to the centroid of UAV 1 and UAV 2 to remain connected with both UAVs. However,

TABLE IV
PATH PLANNER PARAMETERS.

Variable	Value	Description
R (m)	$\{50, 100, 150, 200\}$	Communication range
$\mathbf{p_0^{U_0}}$ (m)	[166.3, 500]	Initial position
$\mathbf{v_0^{U_0}}$ (m/s)	[25, 25]	Initial velocity
$\theta_0^{U_0}$	$45°$	Initial heading angle
v_{min} (m/s)	20	Minimum velocity
v_{max} (m/s)	40	Maximum velocity
ω_{min}	$-30°$	Minimum turn rate
ω_{max}	$30°$	Maximum turn rate
E (Δt)	32	Estimation window
W (Δt)	$\{1, 8\}$	Horizon window

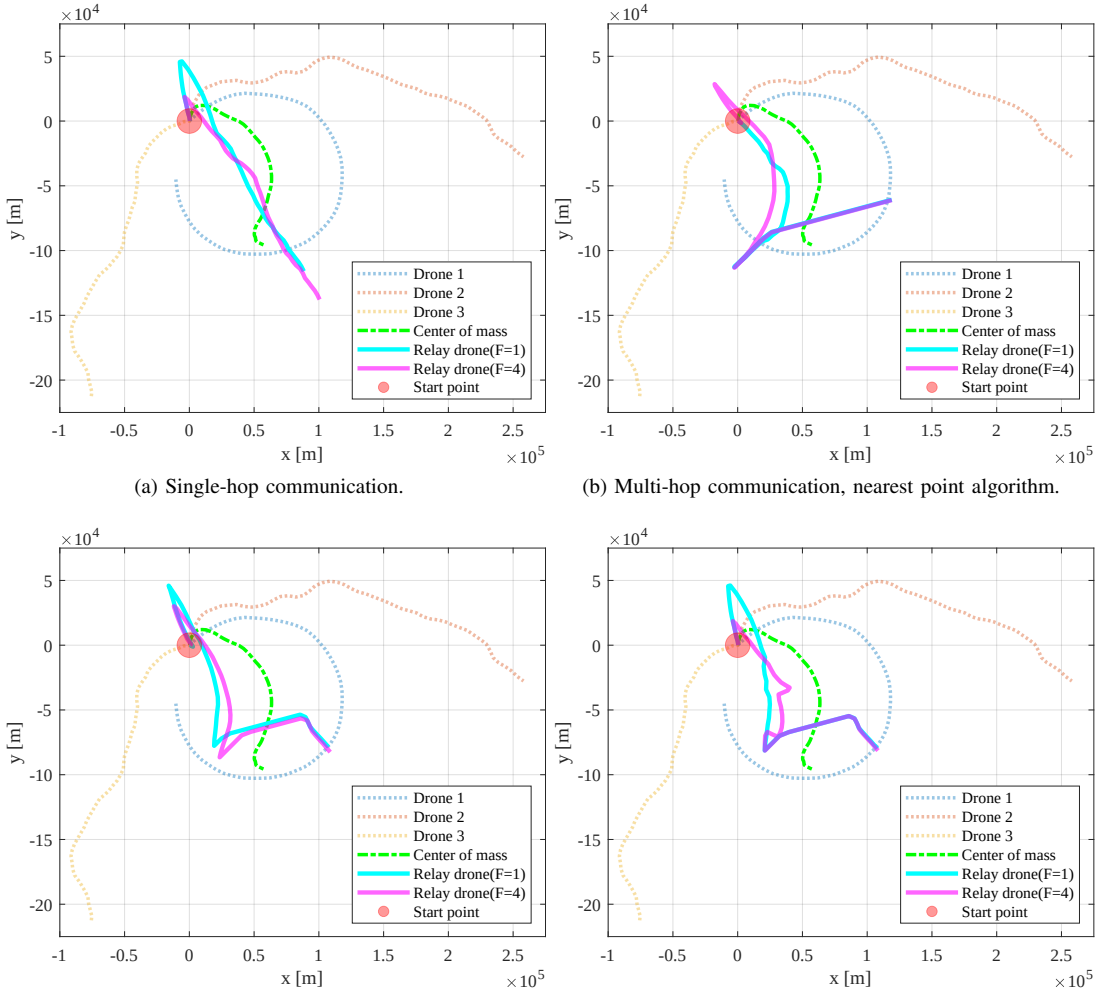

(a) Single-hop communication.

(b) Multi-hop communication, nearest point algorithm.

(c) Multi-hop communication, midpoint algorithm.

(d) Multi-hop communication, hybrid algorithm.

Fig. 5. Simulation results with $R = 100$ km.

the relay UAV relies on UAV 1 to communicate with UAV 3 and does not consider the distance of UAV 3.

The trajectory of the relay UAV is influenced by the midpoint algorithm, which considers the positions of all tracker UAVs. The optimal relay UAV trajectories determined by the algorithm are depicted in Figure 5c. At the start of the simulation, the trajectory is similar to the nearest point algorithm, aiming to be in the center of UAV 3, which is the furthest UAV, and the centroid of UAV 1 and UAV 2. However, before UAV 2 becomes the furthest UAV, the relay UAV adjusts its movement in response to its movement due to the objective function. This is the main difference between the nearest point and midpoint algorithms. Towards the end of the simulation, UAV 3 becomes the furthest UAV again, and the relay UAV moves towards the $x = y$ line. The impact of the optimization horizon is similar to that of the single-hop communication scenario, with more intricate movements when the optimization horizon is taken into account.

In the hybrid algorithm, the trajectory at the beginning is identical to that of the single-hop communication scenario since the relay UAV tries to establish a direct connection with all tracker UAVs. After some time, when the single-hop communication is no longer feasible, it adopts the midpoint objective, and its trajectory is almost identical to the midpoint algorithm. The impact of the horizon window is similar to the earlier scenarios. The trajectory of the relay UAV is shown in Figure 5d.

At the beginning of the simulation, all UAVs are interconnected, and the Mayer term of the optimization determines the trajectory. When the distance between the relay UAV and the tracker UAV reaches the communication range limits, the Bolza term of the problem dominates the objective function. The sharp turns in the trajectory are due to the Mayer term, while the small distortions on the trajectory are results of the Bolza term. The incorporation of an optimization horizon results in increased performance of the path planner. However, there are several issues associated with introducing an optimization horizon. Firstly, the objective function becomes more complex, and the dimensionality increases exponentially with an increase in the horizon window. Moreover, the optimization operates on the estimator results, therefore the optimization horizon cannot exceed the estimation window. Longer horizon windows decrease the precision to dynamic changes in the environment.

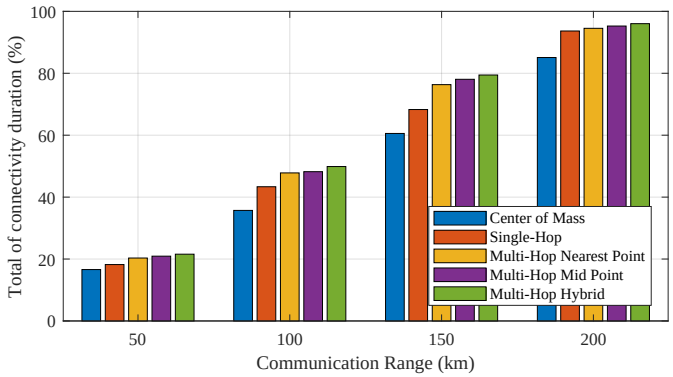

Fig. 6. Total connectivity duration of the proposed algorithms.

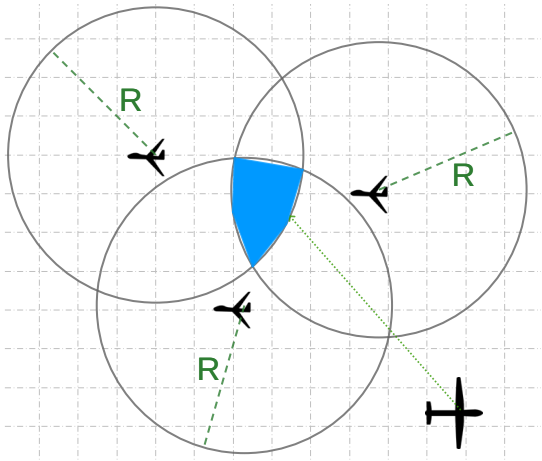

Fig. 7. Connectivity area (blue) for relay UAV to form a single-Hop communication. The communication radius for all UAVs, including the relay UAV, is R. For successful communication, the distance between the relay UAV and any tracker UAV must be less than R. In the scenario with three tracker UAVs and single-hop communication, the relay UAV must be within the transmission circles of all tracker UAVs. This means the relay UAV must be positioned within the intersection area of the three transmission circles to ensure communication with all tracker UAVs.

The single-hop communication method improves the baseline technique by 7.89% in the absence of an optimization horizon and 13.15% with its application. The nearest point algorithm achieves a 36.84% improvement, irrespective of the optimization horizon. The midpoint algorithm leads to an improvement of 42.10% and 35.52% with and without optimization horizon, respectively. Finally, the hybrid algorithm enhances the baseline by 42.10%.

The duration of network connectivity during simulations was calculated for four different communication ranges. Figure 6 illustrates the correlation between the communication range of the UAVs and the connectivity time. It also demonstrates the improvement achieved by the proposed methods compared to the baseline method. For instance, when the communication range is $R = 100$ km, the single-hop communication path planner achieves connectivity for 43.99% of the total simulation time, while the baseline method achieves only 35.71%. Furthermore, the multi-hop communication path planners exhibit better performance. The nearest point algorithm has a connectivity duration of 47.56%, the midpoint algorithm has 48.73%, and the hybrid algorithm has 50.26%.

The present outcomes are inadequate as key performance indicators for evaluating the planners, given that their accuracy is significantly influenced by the extent of communication coverage. In order to mitigate the impact of communication range, the duration of sustained network connectivity is calculated and subsequently compared to the period during which network connectivity is ensured by the relay UAV.

VI. Theoretical Limits on Network Lifetime

In this section, whether the relay UAV can be positioned such that a connected network topology is obtained among all UAVs if the positions of tracker UAVs are exactly known at time t is investigated. For each communication type, a separate geometric problem is formulated.

A. Single-Hop Communication

To have a connected single-hop network, all tracker UAVs have to communicate with relay UAV directly. At time step k, let $d_i^{(x,y)}(k)$ denote the distance between point (x, y) and the tracker UAV i. If the distance $d_i^{(x,y)}(k) \geq R$, the connection link cannot be formed. To call a topology feasible, there at least needs to be one point (x, y) in the map that satisfies $d_i^{(x,y)}(k) \leq R$ for $\forall i = 1, ..., N$.

At each time instance k, circles are formed centered at the positions of tracker UAVs with radius R, and the intersection area between N circles is checked. The sum of these intersection areas over the simulation time gives the maximum duration for which the network can remain connected. Figure 7 illustrates a feasible area for $N = 3$.

B. Multi-Hop Communication

In the case of multi-hop communication, it is necessary to have a connected network graph among the UAVs. However, determining the feasibility of placing the relay UAV to achieve a connected network topology is more complex than in the single-hop communication case. For instance, in some cases, the relay UAV must bridge two subsets of tracker UAVs that are already communicating within the subsets. The objective is to determine if there is a viable area for the relay UAV placement in a multi-hop network with $N = 3$ tracker UAVs. To cover all possible cases, different topology configurations are examined. The aim is to find a feasible area that guarantees a connected topology between the UAVs.

Circular areas with radius R and centers $\mathbf{p}_k^{U_i}$ are drawn to represent the communicable areas for each UAV. It is assumed that any point within the circular area can communicate with UAV i. The distance between tracker UAV i and j is denoted by d_{ij}. It is assumed, without loss of generality, that $d_{12} \leq d_{13} \leq d_{23}$. The distances between the UAVs are compared to the communication range to determine the existence of a feasible area The feasible points must lie within the union of the communicable areas, as the relay UAV will be unable to communicate with any UAVs otherwise.

Three possible scenarios arise when dealing with 3 UAVs: all three are able to communicate, only two are able to

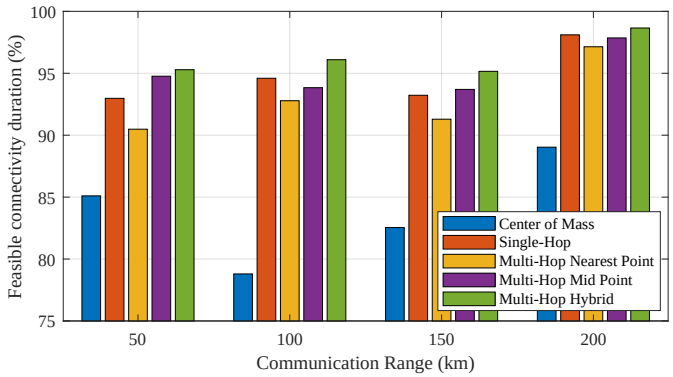

Fig. 8. Relative connectivity duration of the proposed algorithms.

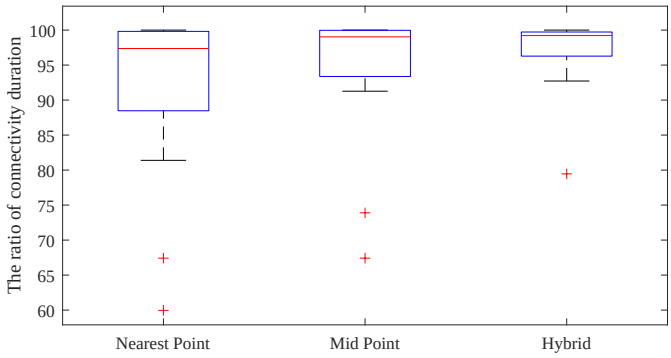

Fig. 9. Box plot of multi-hop algorithms.

communicate, or none are able to communicate. In the case where all three UAVs can communicate, any point within the union of the communicable areas of each UAV is a feasible point for the relay UAV, given that $d_{13} \leq R$. In this scenario, d_{23} does not impact communication since the three UAVs are connected even without the relay UAV. An illustration of the configuration of this case can be seen in Figure 7.

When only 2 UAVs can communicate, it implies that $d_{12} \leq R$ and $d_{13} \geq R$. This case can be further divided into two subcases based on d_{13} being either between R and $2R$ or larger than $2R$. In the former case, the relay UAV can be placed at the intersection area of UAV 1 and UAV 3 to connect both of them, since UAV 1 and UAV 2 are already connected. Consequently, a connected network topology is formed. However, in the latter case, it is impossible to place the relay UAV in a way that connects UAV 1 and UAV 3, and thus a connected network topology cannot be established.

In the event that there is no connection between the UAVs, where the distance between two UAVs is greater than or equal to the communication range, the relay UAV must establish communication with all three UAVs to create a connected network topology. This is equivalent to the process of determining whether a single-hop network can be established between the UAVs, as discussed previously. For two circles to have an intersection area, the distance between their centers should be smaller than the summation of their radii. To have an intersection area between 3 circles, the distance between the circles should satisfy the following inequality $R \leq d_{12} \leq d_{13} \leq d_{23} \leq 2R$. There are two possible cases for this configuration with intersection area and no intersection area.

A feasibility check is carried out for each t, and the duration that the topology can remain connected is determined by summing the results throughout the simulation time to obtain the maximum possible duration. The maximum amount of time that the network can remain connected for each target mobility case and communication range is evaluated. For each algorithm, the ratio between the time the relay UAV maintains network connectivity and the maximum possible duration of network connectivity, called relative connectivity duration, is calculated.

The results in Figure 8 show that both in single-hop and multi-hop communication cases, relative connectivity durations increase with the proposed algorithms compared with the center of mass baseline method. The algorithm for single-hop communication has better results than the nearest point algorithm since the feasible area increases in the multi-hop communication scenario. Although the nearest point algorithm planner has longer connection duration, it is not as relatively successful as the single-hop communication planner in terms of being in the connectivity area.

All three algorithms for the multi-hop communication scenario improves the performance in terms of relative connectivity duration compared to the baseline algorithm. Figure 8 shows that the midpoint algorithm performs better than the nearest point algorithm, and hybrid algorithm performs better than both. Figure 9 presents the statistics of the relative connectivity duration for all simulations for the multi-hop communication. It is observed that among the three algorithms considered, the hybrid algorithm not only achieves the longest connectivity duration, but also has the most robust performance.

VII. Network Topology

The network established in this study operates within the paradigm of Flying Ad Hoc Networks (FANETs), a specialised subclass of Mobile Ad Hoc Networks (MANETs) and Vehicular Ad Hoc Networks (VANETs) [31]. FANETs are characterised by dynamic and rapidly changing network topologies due to the high-speed mobility of UAVs. This rapid mobility leads to frequent alterations in node positions and fluctuations in node load, presenting unique challenges for network design and stability. FANETs are typically supported by UAV-to-UAV data links, allowing them to expand coverage dynamically and flexibly. However, in contrast to other ad hoc networks, FANETs generally exhibit lower node density due to both the spatial distribution of UAVs and their energy constraints.

A key limitation in FANETs arises from the power consumption constraints of UAV hardware, which restricts the number of connections that each UAV can maintain. Furthermore, latency is a critical design factor in FANETs, as in all types of ad hoc networks, and must be considered when determining the network topology. Network lifetime is also essential for FANET performance, especially given that communication hardware in FANETs draws power from the

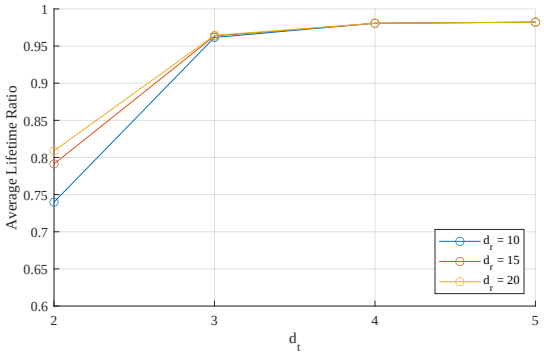

(a) $R = 100$ km.

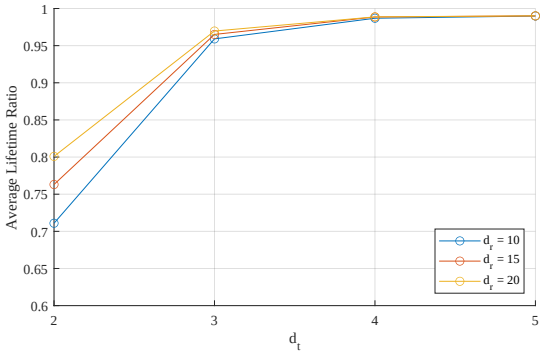

(b) $R = 150$ km.

Fig. 10. Average lifetime ratio as a function of maximum number of tracker and relay UAV connections.

UAV's onboard energy source. Consequently, it is essential to control node degree in order to limit the number of connections each UAV can handle.

In this context, different communication strategies have been evaluated to balance network extensibility with latency reduction. Single-hop communication, similar to a star topology, effectively minimises latency but suffers from limited scalability and resilience due to potential coverage gaps in larger networks. Alternatively, multi-hop communication, akin to a mesh topology, offers enhanced connectivity at the cost of increased latency. Multi-hop communication in FANETs can be approached in two ways: (1) by minimising the number of hops between a tracker UAV and the relay UAV or (2) by minimising the number of nodal connections a UAV maintains. The first approach, while theoretically advantageous, is limited by the autonomous mobility models of tracker UAVs, which prioritise specific target tracking over network-aware routing. The second approach, however, optimises the network by restricting the connection load on both tracker and relay UAVs, which can help extend the network's operational lifetime.

The connection optimization problem shares similarities with the degree-constrained minimum spanning tree problem [32], which is an NP-hard problem. We solved the problem of FANET topology design under nodal degree constraints using the variable neighborhood search [33] which was proposed for the degree constrained spanning tree problem. To demonstrate the potential for extended network lifetime with the proposed algorithms, center of mass algorithm is used as a baseline to explore the effects of the number of connections each UAV can maintain.

The study evaluates 30 randomly generated scenarios with 100 tracker drones with the mobility models presented in Section III-B across two coverage radii: $R = 100$ km and $R = 150$ km. Considering the hardware limitations of typical wireless communication devices used in UAVs, connection limits for the relay UAV, d_r, are set at $d_r = 10$, 15, and 20, while connection limits for tracker UAVs, d_t, are evaluated with 2, 3, 4, and 5. The position of the relay UAV is determined using the center of mass algorithm. Average lifetime ratio which represents the the ratio between the duration network is connected with the degree limitations and the duration network can remain connected without the limitations is used as the performance criteria. For single-hop, there is no limitation on the number of connection the relay UAV can make and tracker UAVs can only be connected directly to relay UAV. These parameters are critical, as they directly influence network durability and performance.

The results of these evaluations, presented in Figure 10a, show that average lifetime ratio of network with single-hop communication is only around 30%, which is substantially lower than the lifetimes achieved under multi-hop communications. For the multi-hop communication, if tracker UAVs can connect up to 4 or 5 UAVs, the connected network topology can be achieved throughout the lifetime that it remains connected. However for $d_t = 2$ and $d_t = 3$, the lifetime of the network is lower. As the proposed algorithms in Section IV-B are shown to perform better compared to center of mass algorithm, proposed algorithms are expected to achieve higher average lifetime ratios under nodal degree constraints compared to results reported in this section.

VIII. Conclusion

In this paper, motion planning for a relay UAV for establishing a connected UAV network topology is investigated, so that each UAV in the network has the ability to communicate with other UAVs. The communication is studied under two scenarios: single-hop and multi-hop. Single-hop communication involves a direct link from the tracking UAVs to the relay UAV, which requires reliable and low delay communication to ensure effective surveillance. On the other hand, in multi-hop communication, the relay UAV can communicate with the other UAVs through intermediate nodes, which increases the duration that the UAVs remain connected to achieve higher resilience. The optimization problems are formulated for both single-hop and multi-hop communication, aiming to maximize the connected time of the network topology.

Center of mass method which selects the trajectory of the relay UAV as the centroid of the three targets at all times is used as the baseline for comparison. The performance of the algorithm used in the single-hop communication shows that the solution with no time horizon shows 13% improvement, while the solution with a time horizon shows 16% improvement over the baseline. The formulation with optimization horizon provides the best results, which is expected since the trajectory is optimized with more knowledge about the tracker UAVs. For the multi-hop communication scenario, trajectories

generated by all proposed algorithms achieve connectivity for a period which is over 90% of the maximum possible duration of having a connected topology. Amongst the proposed three algorithms, the hybrid algorithm is found to be the most effective algorithm with over 95% of the maximum possible network lifetime achieved.

As a future work, heterogeneous UAV systems with coverage and communication ranges can be explored. Additionally, the implementation of multiple relay UAVs can be considered to enhance connectivity. Further research could also investigate adaptive algorithms that respond dynamically to changes in the environment and target behavior, as well as the integration of machine learning techniques to predict target movements and optimize UAV trajectories more effectively.

REFERENCES

[1] Á. Madridano, A. Al-Kaff, D. Martín, and A. de la Escalera, "Trajectory planning for multi-robot systems: Methods and applications," *Expert Systems with Applications*, vol. 173, p. 114660, 2021.

[2] L. Xing, X. Fan, Y. Dong, Z. Xiong, L. Xing, Y. Yang, H. Bai, and C. Zhou, "Multi-UAV cooperative system for search and rescue based on YOLOv5," *International Journal of Disaster Risk Reduction*, vol. 76, p. 102972, 2022.

[3] S. H. Alsamhi, A. V. Shvetsov, S. Kumar, S. V. Shvetsova, M. A. Alhartomi, A. Hawbani, N. S. Rajput, S. Srivastava, A. Saif, and V. O. Nyangaresi, "UAV computing-assisted search and rescue mission framework for disaster and harsh environment mitigation," *Drones*, vol. 6, no. 7, p. 154, 2022.

[4] Y. Tian, K. Liu, K. Ok, L. Tran, D. Allen, N. Roy, and J. P. How, "Search and rescue under the forest canopy using multiple UAVs," *The International Journal of Robotics Research*, vol. 39, no. 10-11, pp. 1201–1221, 2020.

[5] E. Yanmaz, "Joint or decoupled optimization: Multi-UAV path planning for search and rescue," *Ad Hoc Networks*, vol. 138, p. 103018, 2023.

[6] Z. Sun, H. Garcia de Marina, B. D. Anderson, and C. Yu, "Collaborative target-tracking control using multiple fixed-wing unmanned aerial vehicles with constant speeds," *Journal of Guidance, Control, and Dynamics*, vol. 44, no. 2, pp. 238–250, 2021.

[7] X. Shao, J. Zhang, and W. Zhang, "Distributed cooperative surrounding control for mobile robots with uncertainties and aperiodic sampling," *IEEE Transactions on Intelligent Transportation Systems*, vol. 23, no. 10, pp. 18 951–18 961, 2022.

[8] M. Tortonesi, C. Stefanelli, E. Benvegnu, K. Ford, N. Suri, and M. Linderman, "Multiple-UAV coordination and communications in tactical edge networks," *IEEE Communications Magazine*, vol. 50, no. 10, pp. 48–55, 2012.

[9] H. M. La and W. Sheng, "Dynamic target tracking and observing in a mobile sensor network," *Robotics and Autonomous Systems*, vol. 60, no. 7, pp. 996–1009, 2012.

[10] S. Wang, S. Hosseinalipour, M. Gorlatova, C. G. Brinton, and M. Chiang, "UAV-assisted online machine learning over multi-tiered networks: A hierarchical nested personalized federated learning approach," *IEEE Transactions on Network and Service Management*, vol. 20, no. 2, pp. 1847–1865, 2023.

[11] M. A. Khan, N. Kumar, S. A. H. Mohsan, W. U. Khan, M. M. Nasralla, M. H. Alsharif, J. Żywiołek, and I. Ullah, "Swarm of UAVs for network management in 6G: A technical review," *IEEE Transactions on Network and Service Management*, vol. 20, no. 1, pp. 741–761, 2023.

[12] P. Ladosz, H. Oh, and W. Chen, "Prediction of air-to-ground communication strength for relay UAV trajectory planner in urban environments," *IEEE/RSJ International Conference on Intelligent Robots and Systems (IROS)*, pp. 6831–6836, 2017.

[13] P. Ladosz, H. Oh, and W.-H. Chen, "Trajectory planning for communication relay unmanned aerial vehicles in urban dynamic environments," *Journal of Intelligent & Robotic Systems*, vol. 89, no. 1-2, pp. 7–25, 2018.

[14] S. Kim, H. Oh, J. Suk, and A. Tsourdos, "Coordinated trajectory planning for efficient communication relay using multiple UAVs," *Control Engineering Practice*, vol. 29, pp. 42 – 49, 2014.

[15] A. Giagkos, E. Tuci, M. S. Wilson, and P. B. Charlesworth, "UAV flight coordination for communication networks: genetic algorithms versus game theory," *Soft Computing*, vol. 25, no. 14, pp. 9483–9503, 2021.

[16] D. Liu, Y. Xu, J. Wang, Y. Xu, A. Anpalagan, Q. Wu, H. Wang, and L. Shen, "Self-organizing relay selection in UAV communication networks: A matching game perspective," *IEEE Wireless Communications*, vol. 26, no. 6, pp. 102–110, 2019.

[17] D. Liu, J. Wang, K. Xu, Y. Xu, Y. Yang, Y. Xu, Q. Wu, and A. Anpalagan, "Task-driven relay assignment in distributed UAV communication networks," *IEEE Transactions on Vehicular Technology*, vol. 68, no. 11, pp. 11 003–11 017, 2019.

[18] R. S. De Moraes and E. P. De Freitas, "Multi-UAV based crowd monitoring system," *IEEE Transactions on Aerospace and Electronic Systems*, vol. 56, no. 2, pp. 1332–1345, 2019.

[19] N. Sharvari, D. Das, J. Bapat, and D. Das, "Connectivity and collision constrained opportunistic routing for emergency communication using UAV," *Computer Networks*, vol. 220, p. 109468, 2023.

[20] E. Yanmaz, "Positioning aerial relays to maintain connectivity during drone team missions," *Ad Hoc Networks*, vol. 128, p. 102800, 2022.

[21] ——, "Dynamic relay selection and positioning for cooperative UAV networks," *IEEE Networking Letters*, vol. 3, no. 3, pp. 114–118, 2021.

[22] L. Booth, J. Bruck, M. Franceschetti, and R. Meester, "Covering algorithms, continuum percolation and the geometry of wireless networks," *The Annals of Applied Probability*, vol. 13, no. 2, pp. 722–741, 2003.

[23] X. R. Li and V. P. Jilkov, "Survey of maneuvering target tracking. part i. dynamic models," *IEEE Transactions on aerospace and electronic systems*, vol. 39, no. 4, pp. 1333–1364, 2003.

[24] B. Li, Z.-p. Yang, D.-q. Chen, S.-y. Liang, and H. Ma, "Maneuvering target tracking of UAV based on MN-DDPG and transfer learning," *Defence Technology*, vol. 17, no. 2, pp. 457–466, 2021.

[25] M. Eltoukhy, M. O. Ahmad, and M. Swamy, "An adaptive turn rate estimation for tracking a maneuvering target," *IEEE Access*, vol. 8, pp. 94 176–94 189, 2020.

[26] J. Haugen and L. Imsland, "Monitoring moving objects using aerial mobile sensors," *IEEE Transactions on Control Systems Technology*, vol. 24, no. 2, pp. 475–486, 2015.

[27] P. Tyagi, Y. Kumar, and P. Sujit, "NMPC-based UAV 3d target tracking in the presence of obstacles and visibility constraints," in *International Conference on Unmanned Aircraft Systems (ICUAS)*. IEEE, 2021, pp. 858–867.

[28] Y. Kim and H. Bang, "Introduction to kalman filter and its applications," in *Introduction and Implementations of the Kalman Filter*. IntechOpen, 2018.

[29] L. T. Biegler, *Nonlinear programming: concepts, algorithms, and applications to chemical processes*. SIAM, 2010.

[30] R. C. S. Nakano, A. Bandala, G. E. Faelden, J. M. Maningo, and E. P. Dadios, "A genetic algorithm approach to swarm centroid tracking in quadrotor unmanned aerial vehicles," in *International Conference on Humanoid, Nanotechnology, Information Technology, Communication and Control, Environment and Management (HNICEM)*. IEEE, 2014, pp. 1–6.

[31] I. Bekmezci, O. K. Sahingoz, and Ş. Temel, "Flying ad-hoc networks (FANETs): A survey," *Ad Hoc Networks*, vol. 11, no. 3, pp. 1254–1270, 2013.

[32] A. M. de Almeida, P. Martins, and M. C. de Souza, "Min-degree constrained minimum spanning tree problem: complexity, properties, and formulations," *International Transactions in Operational Research*, vol. 19, no. 3, pp. 323–352, 2012.

[33] C. C. Ribeiro and M. C. Souza, "Variable neighborhood search for the degree-constrained minimum spanning tree problem," *Discrete Applied Mathematics*, vol. 118, no. 1-2, pp. 43–54, 2002.

Abdulsamet Dağaşan received the B.S. and M.S. degrees in Electrical and Electronics Engineering from Bilkent University, Ankara, Turkey, in 2017 and 2020, respectively. He is currently pursuing the Ph.D. degree with the Department of Electrical and Electronics Engineering, Bilkent University, Ankara, Turkey. He is also a Senior Software Engineer at Aselsan, Ankara, Turkey. His research interests include wireless communication systems, nonlinear optimization, machine learning, deep learning and UAVs.

Ezhan Karaşan (Member, IEEE) received the B.S. degree from Middle East Technical University, Ankara, Turkey, the M.S. degree from Bilkent University, Ankara, and the Ph.D. degree from Rutgers University, Piscataway, NJ, USA, in 1987, 1990, and 1995, respectively, all in electrical engineering. During 1995–1996, he was a Postdoctorate Researcher with Bell Labs, Holmdel, NJ. From 1996 to 1998, he was a Senior Technical Staff Member with the Lightwave Networks Research Department, AT&T Labs Research, Red Bank, NJ. Since 1998, he has been with the Department of Electrical and Electronics Engineering, Bilkent University, where he is currently a Full Professor. He has participated in FP6-IST Network of Excellence (NoE) e- Photon/ONe+ and FP7-IST NoE BONE projects. His current research interests are in the application of optimization and performance analysis tools for the design, engineering, and analysis of optical and wireless networks.